A

MMP9

GAPDH

Control BAPN BAPN BAPN
              +AngII +NE

B

Pro-MMP9
MMP9

Control BAPN BAPN BAPN
              +AngII +NE

C

H&E   MMP9   Neutrophil   Nonimmune

D

H&E   FIZ   FIZ   DHE
                    +1,10-phenanthroline

Figure 4. AAD in BAPN/AngII-treated wild type (WT) mice is accompanied by enhanced MMP9 expression, neutrophil infiltration, and superoxide production. A, Analysis of *MMP9* mRNA expression by reverse transcription polymerase chain reaction in aortic tissues from the WT mice treated with vehicle (control), BAPN, BAPN/AngII (BAPN+AngII), or BAPN/NE (BAPN+NE). Polymerase chain reaction products of 3 independent samples from each group are shown. B, Gelatinolytic activity of the aortic tissue homogenates was assessed by gelatin zymography. BAPN/AngII-treated WT aorta shows gelatinolytic bands of 92 kDa and 87 kDa, corresponding to pro-MMP9 and active MMP9, respectively. C, Serial paraffin sections of dissected thoracic aorta of BAPN/AngII-treated WT mice were stained with H&E and immunostained with anti-MMP9 antibody, antineutrophil antibody, or control immunoglobulin G. Note the infiltration of MMP9-positive neutrophils in the media of the dissected lesion. D, Film in situ zymography and dihydroethidium staining of aortic tissues from BAPN/AngII-treated or control vehicle-treated WT mice. Serial frozen sections were made and stained with H&E or subjected to film in situ zymography using gelatin films coated with or without 1,10-phenanthroline. Frozen sections were also stained with dihydroethidium. Scale bars, 200 μm. AAD indicates acute aortic dissection; BAPN, β-aminopropionitrile monofumarate; AngII, angiotensin II; WT, wild type; MMP9, matrix metalloproteinase 9; NE, norepinephrine; H&E, hematoxylin and eosin stain; FIZ, film in situ zymography; GAPDH, glyceraldehyde 3-phosphate dehydrogenase; and DHE, dihydroethidium.

thoracic aortas (Figure 5). In control mice treated with BAPN alone or BAPN and NE, immunostaining of MMP9 and neutrophils was only rarely observed in the tissues (Figure 5). These findings suggest that the increased levels of MMP9 detected in the AAD aortas are derived primarily from neutrophils that infiltrate both the aortic intima and media.

Reduction of AAD Incidence by Pharmaceutical and Genetic Depletion of MMP9 or by Neutrophil Depletion

To determine whether MMP9 plays a direct role in the AAD mouse model, BAPN/AngII-treated mice were treated with synthetic MMP inhibitor ONO-4817. As shown in Figure 6A, when ONO-4817 was administered orally on daily basis to BAPN-treated WT mice from 48 hours prior to AngII

infusion until sacrifice, the incidence of AAD decreased significantly from 100% to 60%, and spontaneous death caused by aortic rupture was blocked completely. Consistent with these observations, when *MMP9*^{-/-} mice were treated with BAPN/AngII, AAD incidence was attenuated remarkably to basal levels (10% of the *MMP9*^{-/-} mice) whereas BAPN alone induced thoracic aneurysm formation at a frequency comparable with that observed in WT mice (Figure 6A and 6B). Hence, these findings support a direct role for MMP9 in the development of AAD.

Although multiple cell populations are capable of expressing MMP9 (eg, macrophages,[12] endothelial cells,[26] and vascular smooth muscle cells[24]), neutrophil infiltrates dominated the affected tissues. As such, we depleted neutrophils during aneurysm formation by treating the mice with anti-Gr-1
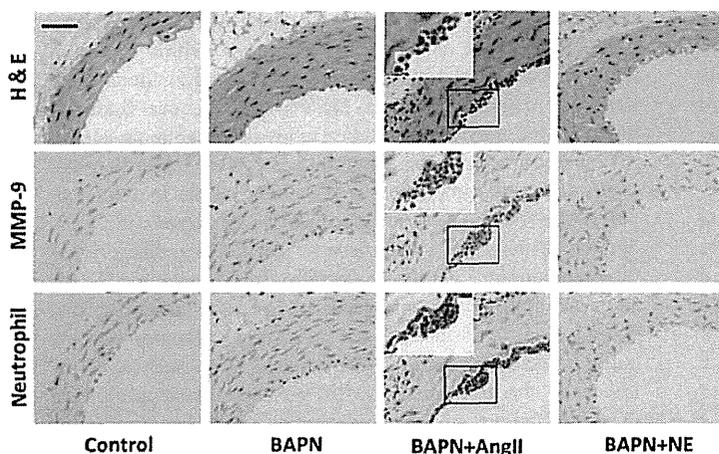

Figure 5. Infiltration of MMP9-positive neutrophils in the intima of nondissected lesions of BAPN/AngII-induced AAD thoracic aortas. MMP9 expression and neutrophil infiltration were examined by histology and immunohistochemistry in the aortas of untreated wild type mice (control) or wild type mice treated with BAPN alone, BAPN+AngII, and BAPN+NE. Note the accumulated MMP9-positive neutrophils in the intima of nondissected aorta from BAPN/AngII-treated mice. Inlets in the BAPN+AngII group show a higher-power view of the rectangular areas. Scale bar, 200 μm. MMP9 indicates matrix metalloproteinase 9; H&E, hematoxylin and eosin stain; BAPN, β-aminopropionitrile monofumarate; AngII, angiotensin II; AAD, acute aortic dissection; and NE, norepinephrine.
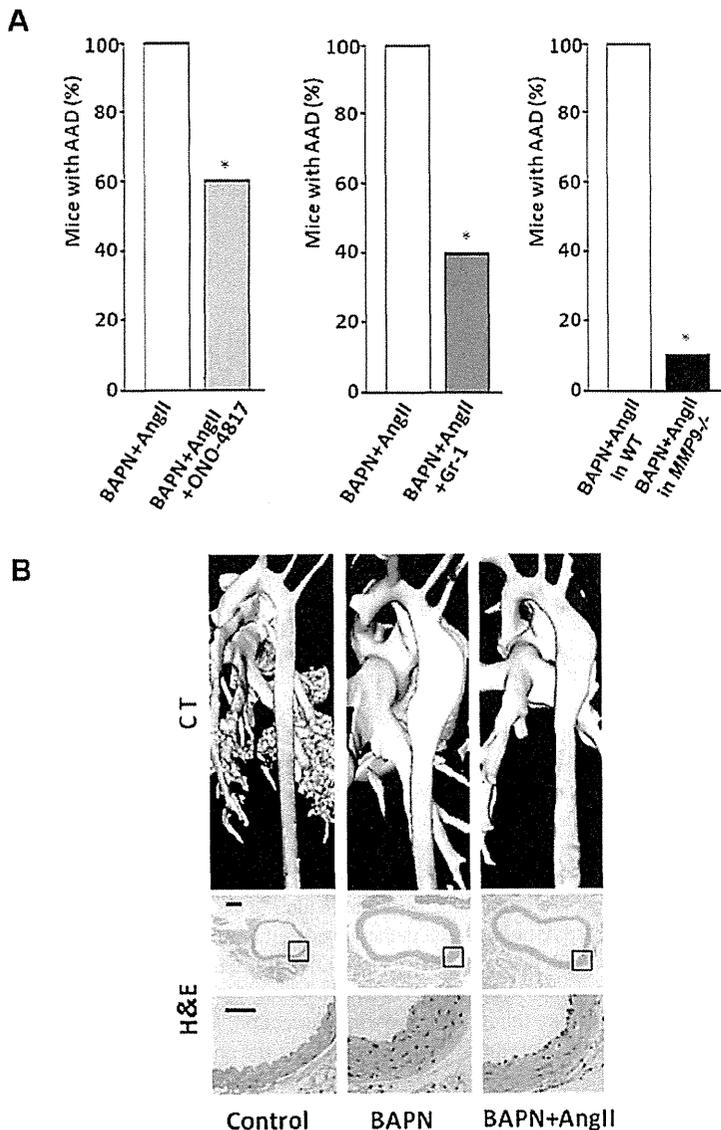
Figure 6. Pharmaceutical and genetic depletion of MMP9 or immunological depletion of neutrophils attenuates AAD incidence in mice. A, AAD incidence in BAPN/AngII-treated WT mice that were treated with ONO-4817 (BAPN+AngII+ONO-4817) (left) or anti-Gr-1 antibody (BAPN+AngII+Gr-1) (middle) and the incidence in BAPN/AngII-treated $MMP9^{-/-}$ mice (right) were compared with that in BAPN/AngII-treated WT mice (n=10 for each group). The probability value was adjusted with the Bonferroni method for pairwise comparisons. *$P<0.05$ versus BAPN/AngII-treated WT mice. B, Three-dimensional images of enhanced computed tomographic scan (upper) and histology (middle and bottom) of the aortas from $MMP9^{-/-}$ mice that were treated with vehicle for 4 weeks (control), BAPN alone for 4 weeks (BAPN), or BAPN for 4 weeks and then AngII for 24 hours (BAPN+AngII). Note that AAD formation is blocked in BAPN/AngII-treated $MMP9^{-/-}$ mice. (Bottom) High-power view of the rectangular areas in the middle panel. Scale bars, 200 μm and 100 μm for the middle and bottom panels, respectively. MMP9 indicates matrix metalloproteinase 9; AAD, acute aortic dissection; BAPN, β-aminopropionitrile monofumarate; AngII, angiotensin II; anti-Gr-1, anti-granulocyte-differentiation antigen-1; WT, wild type; and H&E, hematoxylin and eosin stain.

neutralizing antibody. The number of circulating neutrophils was reduced to 20% of control levels by intraperitoneal injection of the antibody for 48 hours prior to AngII infusion (data not shown), and, as expected, neutrophil depletion attenuated AAD incidence significantly (Figure 6A).

AngII-Induced Neutrophil Infiltration to Aortic Intima Independent From MMP9 Expression

Infiltration of neutrophils into the aortic intima was observed in BAPN/AngII-treated WT mice with or without ONO-4817 administration, as well as in BAPN/AngII-treated $MMP9^{-/-}$ mice (Figure 7A). Hence, these data demonstrate that AngII promotes neutrophil infiltration independent of MMP9 expression in our AAD model, but these results do not exclude the possibility that normal rates of neutrophil infiltration are maintained only within the noncross-linked, fragile vessel wall caused by chronic BAPN treatment. Thus, we further assessed the effect of AngII on neutrophil infiltration by

infusing AngII in BAPN-untreated WT or $MMP9^{-/-}$ mice wherein vascular structural integrity is intact. As shown in Figure 7B, neutrophil infiltration into the aortic intima was unaffected between the 2 groups, indicating that AngII infusion evokes neutrophil infiltration to the intact aortic wall independent of MMP9 expression.

Discussion

In the current study, we demonstrated that serum levels of MMP9 and AngII are elevated in AAD patients, but not in patient populations with chronic, nonruptured aneurysms. Furthermore, increased circulating levels of MMP9 correlated with the presence of MMP9-positive neutrophils that accumulated in the aortic tissues of AAD patients. Given these findings from studies of human AAD specimens, we established a novel mouse model that develops AAD unfailingly within 24 hours of AngII infusion. This model was dependent on preconditioning mouse aortas with the lysyl oxidase
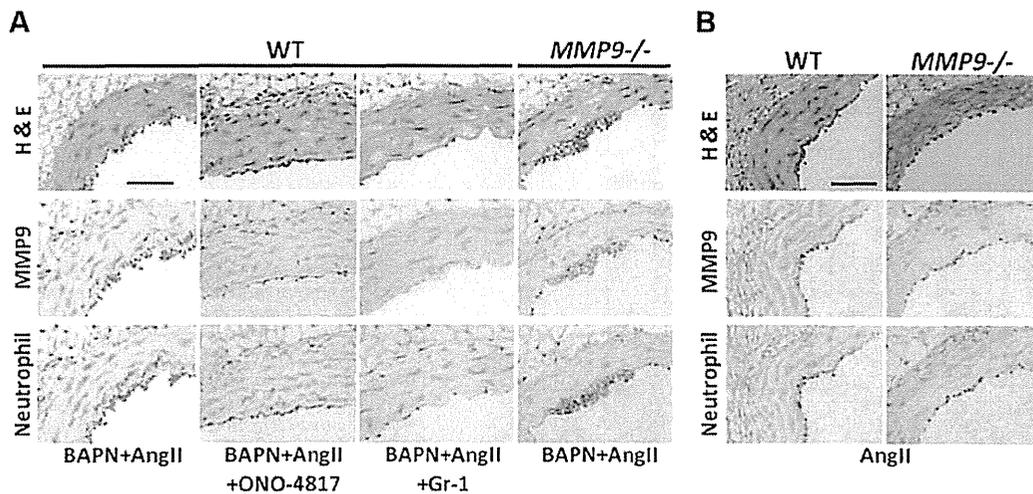
145

Figure 7. AngII-induced neutrophil infiltration in aortic intima is independent of MMP9 expression or BAPN treatment. A, Histological and immunohistochemical analyses of MMP9 expression and neutrophil infiltration in the aortic intima of the WT mice treated with BAPN and AngII (BAPN+AngII); BAPN, AngII, and ONO-4817 (BAPN+AngII+ONO-4817); or BAPN, AngII, and anti-Gr-1 antibody (BAPN+AngII+Gr-1); and those in the intima of the MMP9$^{-/-}$ mice treated with BAPN and AngII (BAPN+AngII) (n=10 for each group). Note that neutrophil infiltration is independent of MMP9 expression. Scale bar, 200 μm. B, Histological and immunohistochemical analyses of MMP9 expression and neutrophil infiltration in the aortic tissues of BAPN-untreated WT and MMP9$^{-/-}$ mice 24 hours after AngII infusion. Note that neutrophil infiltration is independent of BAPN treatment. Scale bar, 200 μm. AngII indicates angiotensin II; WT, wild type; MMP9, matrix metalloproteinase 9; H&E, hematoxylin and eosin stain; BAPN, β-aminopropionitrile monofumarate; and anti-Gr-1, anti-granulocyte-differentiation antigen-1.

inhibitor BAPN to create an aneurysmal, pre-AAD status in immature mice. Collagen and elastin cross-links, which are critical for maintaining vessel wall integrity, are disrupted by BAPN administration,[27] leading to the generation of mechanically fragile aortas that both display medial degeneration and develop aortic aneurysms. This type of aortic aneurysm is typically seen in human connective tissue diseases such as Marfan syndrome,[28] but the histology of cystic medial degeneration is commonly seen in aneurysms that arise secondary to aging and atherosclerosis as well.[3,4] It is not clearly elucidated whether aortic matrix cross-links are different between normal and aneurysmal aorta[29]; however, several studies from human pathological samples indicate that the composition of the aortic extracellular matrix changes as medial degeneration proceeds with enhanced deposition of proteoglycans and decreased collagen content, coupled with apoptosis of vascular smooth muscle cells.[30] These findings suggest that the aortic media and its matrix components are disorganized as a function of disease progression, thus leading to the generation of an aneurysmal aorta with weakened mechanical properties. As such, our mouse model would appear to recapitulate a similar state in which suitable triggers, such as AngII, precipitate the transition from a preconditioned, chronic aortic aneurysm to AAD.

Previous studies have suggested possible roles for MMP9 in the development of chronic atherosclerosis-derived aneurysms as well as connective tissue disease-related aortic aneurysm.[31–33] By contrast, our findings demonstrate that AAD formation itself proceeds in an MMP9-dependent fashion that is inhibited significantly by either pharmacological or genetic targeting of MMP9. A previous study by Gough et al[12] has shown that macrophages overexpressing autoactivating MMP9 induce atherosclerotic plaque rupture by disruptions of fibrous cap in apolipoprotein E mice, suggesting the ability of

MMP9 to destroy aortic tissue. Altogether, these data support the notion that MMP9 is responsible for triggering aortic dissection from the preconditioned aneurysmal aorta. We have further demonstrated that neutrophil infiltration is observed in the intima of the predissecting aorta as well as in the dissected media, and that neutrophil depletion attenuates AAD incidence significantly. The importance of inflammation in the pathogenesis of vascular diseases is well documented, but until now, it has been difficult to determine whether neutrophil accumulation triggers dissection or occurs as a consequence of the massive vascular damage that develops during dissection. Because MMP9-positive neutrophils were confined to the intima of nondissected lesions while the dissected lesions displayed strong staining for MMP9-positive neutrophils primarily within the media, we posit that neutrophils infiltrate the intima at the initiation of dissection. Despite the importance of neutrophils, we cannot rule out the contribution of other immune effector cells that might be recruited subsequent to the inflammatory responses initiated by infiltrating neutrophils, as depleting neutrophils attenuated AAD, but not to the degree observed with MMP9 targeting. Indeed, the upregulated MMP9 mRNA levels detected in AAD aortic samples 24 hours after AngII infusion could result from nonneutrophil effector cells, because neutrophil MMP9 synthesis is mostly completed at earlier stages of differentiation, with mature neutrophils primarily storing MMP9 in granule compartments.[34] Nevertheless, the rapid induction of aortic dissection in our model as early as 6 hours after AngII infusion, in tandem with the accumulation of MMP9-positive neutrophils, supports the conclusion that infiltrating neutrophils trigger the initiation of dissection directly or indirectly.

MMP9 is a multifunctional proteinase endowed with the ability to degrade multiple extracellular matrix macromolecules, including types III, IV, and V collagens; denatured

collagens (ie, gelatin); and elastin.[11,35] Furthermore, MMP9 can modulate inflammatory responses by hydrolyzing a variety of cytokines and chemokines.[36] For example, MMP9 can activate prointerleukin-1,[37] increase the bioactivity of interleukin 8,[38] and promote interleukin 13-induced pulmonary inflammation,[39] while inactivating neutrophil chemokines such as growth-regulated oncogene and mature interleukin 1.[37,38] A recent clinical trial has shown that the treatment of aortic abdominal aneurysms with doxycycline, a nonspecific MMP inhibitor, reduced neutrophil and cytotoxic T-cell infiltration into the aneurysmal wall in association with decreased production of MMP9 and inflammatory cytokines.[40] MMP9 has also been reported to affect neutrophil chemotactic activity in lung injury models.[41,42] In the current study, however, we detected no differences in neutrophil infiltration within the aortic tissues of OND-4817-treated mice or between WT and $MMP9^{-/-}$ mice in our AAD model. Furthermore, in contrast to malignant cells, with MMP-dependent invasive activity that is affected by collagen cross-links,[43] our study showed that neutrophils infiltrate aortic tissues similarly in both BAPN-treated and -untreated mice. Together, these data suggest that neutrophil infiltration proceeds independently of MMP9 activity or collagen cross-links in this model system.

A detailed mechanism regarding how MMP9 contributes to the initiation of AAD remains to be defined. In recent studies using $Fibrillin1^{-/-}$ mice, which develop AAD spontaneously secondary to connective tissue defect, the elevation of transforming growth factor levels and its downstream signaling cascade contribute to the pathogenesis of aortic aneurysm and dissection.[44] In this model, MMP2 and MMP9 were both upregulated, and doxycycline attenuated disease progression.[31,32] Because MMP9 is a potent activator of latent transforming growth factor,[45] it is interesting to speculate that upregulated MMP9 activity may trigger AAD by in situ activation of transforming growth factor in the affected aortic media of the mice.

Last, our study has validated AngII as a potent inducer of mouse AAD, a result that complements the higher levels of AngII detected in our AAD patient population. Long-term AngII infusion is known to lead to spontaneous aortic dissection in atherosclerosis models using $apoE^{-/-}$ mice.[46] Recent studies have also demonstrated that Losartan, an antagonist of the AngII receptor, AT1, prevents aortic aneurysm development and aortic root dilation in Marfanoid mice and humans.[44,47] It is clear that the role of AngII in the induction of AAD is not a result of vasopressor effects alone, because NE failed to trigger AAD in our model despite similar levels of hypertension. One of the significant differences between the aortic lesions observed in BAPN/AngII-treated versus BAPN/NE-treated WT mice was the presence of neutrophil infiltrates in the BAPN/AngII-treated mice, suggesting that AngII acts as a potent stimulus for neutrophil infiltration into the aorta intima. Indeed, recent studies indicate that AngII can induce neutrophil infiltration.[22,23] In addition, AngII is also able to activate neutrophils and stimulate the nicotinamide adenine dinucleotide phosphate (NADPH) oxidase-dependent production of reactive oxygen metabolites, which may promote the oxidative autoactivation

of pro-MMP9.[48,49] In the current study, we could show the gelatinolytic metalloproteinase activity and superoxide production in the neutrophil-infiltrated dissecting aortic tissue from the BAPN/AngII-treated mice. Thus, AngII likely plays a key role in triggering AAD onset not only by attracting neutrophils to the affected sites, but also by stimulating the release and activation of pro-MMP9.

This study has a few limitations. First, we used a mouse model to demonstrate the role of neutrophil-derived MMP9 activity in AAD formation. Because mouse models do not recapitulate human disease progression stringently, the results of our AAD model may be different in humans. In the mouse model, AAD was induced in the descending thoracic aorta by AngII infusion to the young mice treated with BAPN. Preconditioning for the AAD induction (ie, aneurism formation) by BAPN treatment is artificial and may be applicable for AAD in patients with connective tissue disorders but not for commonly observed AAD in humans, such as our patients in the current study. Another limitation of this study is that the activation mechanism of pro-MMP9 within aortic tissues has not been examined in mouse or human AAD. Although our study on the mouse model has suggested possible involvement of reactive oxygen species in the activation, detailed studies regarding whether pro-MMP9 activation and AAD incidence are suppressed by antioxidant therapy, and which reactive oxygen species are required for pro-MMP9 activation in coculture system of neutrophils and smooth muscle cells, will be necessary. Moreover, reactive oxygen species-mediated pro-MMP9 activation in human aortic tissues from AAD patients needs to be investigated by future work.

AAD is a potentially fatal disease, the prompt diagnosis and treatment of which are required for successful intervention. Although the fibrin product, D-dimer, is the only established biomarker for AAD, the differential diagnosis of AMI versus pulmonary embolism, which displays similar symptoms to that of AAD, can be difficult.[50,51] In this context, MMP9 could serve as a potential biomarker for the diagnosis of AAD. Furthermore, although the dominant treatment for AAD relies on surgical reinforcement of the affected aorta, our data raise the possibility that the preventive administration of AngII receptor blockers or MMP9-specific inhibitors to patients at risk with nonruptured atherosclerotic aneurysm could prove useful as effective therapeutics to reduce AAD incidence.

Sources of Funding

Disclosures
None.

References
1. Golledge J, Eagle KA. Acute aortic dissection. *Lancet*. 2008;372:55–66.
2. Pretre R, Von Segesser LK. Aortic dissection. *Lancet*. 1997;349:1461–1464.

3. Schlatmann TJ, Becker AE. Histologic changes in the normal aging aorta: implications for dissecting aortic aneurysm. *Am J Cardiol.* 1977;39: 13–20.

4. Carlson RG, Lillehei CW, Edwards JE. Cystic medial necrosis of the ascending aorta in relation to age and hypertension. *Am J Cardiol.* 1970;25:411–415.

5. Eldadah ZA, Brenn T, Furthmayr H, Dietz HC. Expression of a mutant human fibrillin allele upon a normal human or murine genetic background recapitulates a Marfan cellular phenotype. *J Clin Invest.* 1995;95: 874–880.

6. Maki JM, Rasanen J, Tikkanen H, Sormunen R, Makikallio K, Kivirikko KI, Soininen R. Inactivation of the lysyl oxidase gene *Lox* leads to aortic aneurysms, cardiovascular dysfunction, and perinatal death in mice. *Circulation.* 2002;106:2503–2509.

7. Kumar D, Trent MB, Boor PJ. Allylamine and beta-aminopropionitrile induced aortic medial necrosis: mechanisms of synergism. *Toxicology.* 1998;125:107–115.

8. Page RC, Benditt EP. Molecular diseases of connective and vascular tissues: 3. The aldehyde content of normal and lathyritic soluble collagen. *Lab Invest.* 1968;18:124–130.

9. Galis ZS, Sukhova GK, Lark MW, Libby P. Increased expression of matrix metalloproteinases and matrix degrading activity in vulnerable regions of human atherosclerotic plaques. *J Clin Invest.* 1994;94: 2493–2503.

10. Newby AC. Metalloproteinases and vulnerable atherosclerotic plaques. *Trends Cardiovasc Med.* 2007;17:253–258.

11. Katsuda S, Okada Y, Imai K, Nakanishi I. Matrix metalloproteinase-9 (92-kd gelatinase/type IV collagenase equals gelatinase B) can degrade arterial elastin. *Am J Pathol.* 1994;145:1208–1218.

12. Gough PJ, Gomez IG, Wille PT, Raines EW. Macrophage expression of active MMP-9 induces acute plaque disruption in apoE-deficient mice. *J Clin Invest.* 2006;116:59–69.

13. Loftus IM, Naylor AR, Goodall S, Crowther M, Jones L, Bell PR, Thompson MM. Increased matrix metalloproteinase-9 activity in unstable carotid plaques: a potential role in acute plaque disruption. *Stroke.* 2000; 31:40–47.

14. Wilson WR, Anderton M, Schwalbe EC, Jones JL, Furness PN, Bell PR, Thompson MM. Matrix metalloproteinase-8 and -9 are increased at the site of abdominal aortic aneurysm rupture. *Circulation.* 2006;113: 438–445.

15. Nagashima H, Uto K, Sakomura Y, Aoka Y, Sakuta A, Aomi S, Hagiwara N, Kawana M, Kasanuki H. An angiotensin-converting enzyme inhibitor, not an angiotensin II type-1 receptor blocker, prevents beta-aminopropionitrile monofumarate-induced aortic dissection in rats. *J Vasc Surg.* 2002;36: 818–823.

16. Shimizu-Hirota R, Sasamura H, Kuroda M, Kobayashi E, Hayashi M, Saruta T. Extracellular matrix glycoprotein biglycan enhances vascular smooth muscle cell proliferation and migration. *Circ Res.* 2004;94: 1067–1074.

17. Hariya A, Takazawa K, Yamamoto T, Amano A. ONO-4817, a novel matrix metalloproteinase inhibitor, attenuates allograft vasculopathy in a rat cardiac transplant. *J Heart Lung Transplant.* 2004;23: 1163–1169.

18. Shirahane K, Yamaguchi K, Koga K, Watanabe M, Kuroki S, Tanaka M. Hepatic ischemia/reperfusion injury is prevented by a novel matrix metalloproteinase inhibitor, ONO-4817. *Surgery.* 2006;139:653–664.

19. Yamada A, Uegaki A, Nakamura T, Ogawa K. ONO-4817, an orally active matrix metalloproteinase inhibitor, prevents lipopolysaccharide-induced proteoglycan release from the joint cartilage in guinea pigs. *Inflamm Res.* 2000;49:144–146.

20. Nozawa H, Chiu C, Hanahan D. Infiltrating neutrophils mediate the initial angiogenic switch in a mouse model of multistage carcinogenesis. *Proc Natl Acad Sci U S A.* 2006;103:12493–12498.

21. Daugherty A, Manning MW, Cassis LA. Angiotensin II promotes atherosclerotic lesions and aneurysms in apolipoprotein E-deficient mice. *J Clin Invest.* 2000;105:1605–1612.

22. Abu Nabah YN, Losada M, Estelles R, Mateo T, Company C, Piqueras L, Lopez-Gines C, Sarau H, Cortijo J, Morcillo EJ, Jose PJ, Sanz MJ. CXCR2 blockade impairs angiotensin II-induced CC chemokine synthesis and mononuclear leukocyte infiltration. *Arterioscler Thromb Vasc Biol.* 2007;27:2370–2376.

23. Arndt PG, Young SK, Poch KR, Nick JA, Falk S, Schrier RW, Worthen GS. Systemic inhibition of the angiotensin-converting enzyme limits lipopolysaccharide-induced lung neutrophil recruitment through both bra-

24. dykinin and angiotensin II-regulated pathways. *J Immunol.* 2006;177: 7233–7241.

24. Guo RW, Yang LX, Wang H, Liu B, Wang L. Angiotensin II induces matrix metalloproteinase-9 expression via a nuclear factor-kappaB-dependent pathway in vascular smooth muscle cells. *Regul Pept.* 2008; 147:37–44.

25. Szocs K, Lassegue B, Sorescu D, Hilenski LL, Valppu L, Couse TL, Wilcox JN, Quinn MT, Lambeth JD, Griendling KK. Upregulation of Nox-based NAD(P)H oxidases in restenosis after carotid injury. *Arterioscler Thromb Vasc Biol.* 2002;22:21–27.

26. Mauro A, Buscemi M, Gerbino A. Immunohistochemical and transcriptional expression of matrix metalloproteinases in full-term human umbilical cord and human umbilical vein endothelial cells. *J Mol Histol.* 2010;41:367–377.

27. Bruel A, Ortoft G, Oxlund H. Inhibition of cross-links in collagen is associated with reduced stiffness of the aorta in young rats. *Atherosclerosis.* 1998;140:135–145.

28. Schlatmann TJ, Becker AE. Pathogenesis of dissecting aneurysm of aorta: comparative histopathologic study of significance of medial changes. *Am J Cardiol.* 1977;39:21–26.

29. Gaetani P, Tartara F, Grazioli V, Tancioni F, Infuso L, Rodriguez y Baena R. Collagen cross-linkage, elastolytic and collagenolytic activities in cerebral aneurysms: a preliminary investigation. *Life Sci.* 1998;63: 285–292.

30. Tang PC, Coady MA, Lovoulos C, Dardik A, Aslan M, Elefteriades JA, Tellides G. Hyperplastic cellular remodeling of the media in ascending thoracic aortic aneurysms. *Circulation.* 2005;112:1098–1105.

31. Chung AW, Au Yeung K, Sandor GG, Judge DP, Dietz HC, van Breemen C. Loss of elastic fiber integrity and reduction of vascular smooth muscle contraction resulting from the upregulated activities of matrix metalloproteinase-2 and -9 in the thoracic aortic aneurysm in Marfan syndrome. *Circ Res.* 2007;101:512–522.

32. Chung AW, Yang HH, Radomski MW, van Breemen C. Long-term doxycycline is more effective than atenolol to prevent thoracic aortic aneurysm in Marfan syndrome through the inhibition of matrix metalloproteinase-2 and -9. *Circ Res.* 2008;102:e73–e85.

33. McMillan WD, Pearce WH. Increased plasma levels of metalloproteinase-9 are associated with abdominal aortic aneurysms. *J Vasc Surg.* 1999;29: 122–127; discussion 127–129.

34. Borregaard N, Sehested M, Nielsen BS, Sengelov H, Kjeldsen L. Biosynthesis of granule proteins in normal human bone marrow cells: gelatinase is a marker of terminal neutrophil differentiation. *Blood.* 1995;85: 812–817.

35. Okada Y, Gonoji Y, Naka K, Tomita K, Nakanishi I, Iwata K, Yamashita K, Hayakawa T. Matrix metalloproteinase 9 (92-kDa gelatinase/type IV collagenase) from HT 1080 human fibrosarcoma cells: purification and activation of the precursor and enzymic properties. *J Biol Chem.* 1992; 267:21712–21719.

36. Parks WC, Wilson CL, Lopez-Boado YS. Matrix metalloproteinases as modulators of inflammation and innate immunity. *Nat Rev Immunol.* 2004;4:617–629.

37. Schonbeck U, Mach F, Libby P. Generation of biologically active IL-1 beta by matrix metalloproteinases: a novel caspase-1-independent pathway of IL-1 beta processing. *J Immunol.* 1998;161:3340–3346.

38. Van den Steen PE, Proost P, Wuyts A, Van Damme J, Opdenakker G. Neutrophil gelatinase B potentiates interleukin-8 tenfold by aminoterminal processing, whereas it degrades CTAP-III, PF-4, and GRO-alpha and leaves RANTES and MCP-2 intact. *Blood.* 2000;96: 2673–2681.

39. Lanone S, Zheng T, Zhu Z, Liu W, Lee CG, Ma B, Chen Q, Homer RJ, Wang J, Rabach LA, Rabach ME, Shipley JM, Shapiro SD, Senior RM, Elias JA. Overlapping and enzyme-specific contributions of matrix metalloproteinases-9 and -12 in IL-13-induced inflammation and remodeling. *J Clin Invest.* 2002;110:463–474.

40. Lindeman JH, Abdul-Hussien H, van Bockel JH, Wolterbeek R, Kleemann R. Clinical trial of doxycycline for matrix metalloproteinase-9 inhibition in patients with an abdominal aneurysm: doxycycline selectively depletes aortic wall neutrophils and cytotoxic T cells. *Circulation.* 2009;119:2209–2216.

41. Albaiceta GM, Gutierrez-Fernandez A, Parra D, Astudillo A, Garcia-Prieto E, Taboada F, Fueyo A. Lack of matrix metalloproteinase-9 worsens ventilator-induced lung injury. *Am J Physiol Lung Cell Mol Physiol.* 2008;294:L535–L543.

42. Keck T, Balcom JH, Fernandez-del Castillo C, Antoniu BA, Warshaw AL. Matrix metalloproteinase-9 promotes neutrophil migration and

alveolar capillary leakage in pancreatitis-associated lung injury in the rat. *Gastroenterology.* 2002;122:188–201.

43. Sabeh F, Shimizu-Hirota R, Weiss SJ. Protease-dependent versus -independent cancer cell invasion programs: three-dimensional amoeboid movement revisited. *J Cell Biol.* 2009;185:11–19.

44. Habashi JP, Judge DP, Holm TM, Cohn RD, Loeys BL, Cooper TK, Myers L, Klein EC, Liu G, Calvi C, Podowski M, Neptune ER, Halushka MK, Bedja D, Gabrielson K, Rifkin DB, Carta L, Ramirez F, Huso DL, Dietz HC. Losartan, an AT1 antagonist, prevents aortic aneurysm in a mouse model of Marfan syndrome. *Science.* 2006;312:117–121.

45. Yu Q, Stamenkovic I. Cell surface-localized matrix metalloproteinase-9 proteolytically activates TGF-beta and promotes tumor invasion and angiogenesis. *Genes Dev.* 2000;14:163–176.

46. Saraff K, Babamusta F, Cassis LA, Daugherty A. Aortic dissection precedes formation of aneurysms and atherosclerosis in angiotensin II-infused, apolipoprotein E-deficient mice. *Arterioscler Thromb Vasc Biol.* 2003;23:1621–1626.

47. Brooke BS, Habashi JP, Judge DP, Patel N, Loeys B, Dietz HC, III. Angiotensin II blockade and aortic-root dilation in Marfan's syndrome. *N Engl J Med.* 2008;358:2787–2795.

48. El Bekay R, Alvarez M, Monteseirin J, Alba G, Chacon P, Vega A, Martin-Nieto J, Jimenez J, Pintado E, Bedoya FJ, Sobrino F. Oxidative stress is a critical mediator of the angiotensin II signal in human neutrophils: involvement of mitogen-activated protein kinase, calcineurin, and the transcription factor NF-kappaB. *Blood.* 2003;102:662–671.

49. Weiss SJ, Peppin G, Ortiz X, Ragsdale C, Test ST. Oxidative autoactivation of latent collagenase by human neutrophils. *Science.* 1985;227:747–749.

50. Eggebrecht H, Naber CK, Bruch C, Kroger K, von Birgelen C, Schmermund A, Wichert M, Bartel T, Mann K, Erbel R. Value of plasma fibrin D-dimers for detection of acute aortic dissection. *J Am Coll Cardiol.* 2004;44:804–809.

51. Weber T, Hogler S, Auer J, Berent R, Lassnig E, Kvas E, Eber B. D-dimer in acute aortic dissection. *Chest.* 2003;123:1375–1378.

CLINICAL PERSPECTIVE

Acute aortic dissection (AAD) is a potentially fatal vascular disease, and prompt diagnosis and treatment by timely surgery are required for survival of the patients. No efficient biomarkers are available for diagnosis of AAD prior to determination of the disease by computed tomography. Medial degeneration is known as an important risk factor for the development of AAD; however, the emergent nature of the disease and the paucity of animal models prevent us from studying the molecular mechanisms for triggering the disease. We found that matrix metalloproteinase 9 (MMP9) and angiotensin II were increased significantly in blood samples from AAD patients compared with those from normal subjects and the patients with nonruptured aortic aneurysm. This was accompanied by enhanced infiltrations of MMP9-producing neutrophils in the dissected aortas. Based on the data, we established a mouse model of AAD, which was induced by infusion of angiotensin II to mice pretreated with β-aminopropionitrile monofumarate (a lysyl oxidase inhibitor). All mice exhibited AAD within 24 hours after angiotensin II infusion. Aortic tissue from the AAD mice showed enhanced expression and activity of MMP9, and MMP9-immunoreactive neutrophils were infiltrated in both dissected media and intima of nondissected lesions. Genetic depletion or pharmaceutical inhibition of MMP9 and neutrophil ablation attenuated the AAD incidence. These data demonstrate that neutrophil-derived MMP9 is responsible for triggering AAD in this model. Taken together, MMP9 could serve as a potential biomarker for diagnostic screening of AAD, and administration of angiotensin II receptor blockers or MMP9 inhibitors could be effective therapeutic approaches to AAD.

Total Arch Replacement Under Flow Monitoring During Selective Cerebral Perfusion Using a Single Pump

Hideyuki Shimizu, MD, PhD, Toru Matayoshi, CP, Masanori Morita, CP, Toshihiko Ueda, MD, PhD, and Ryohei Yozu, MD, PhD

Departments of Cardiovascular Surgery and Bioengineering, Keio University, Tokyo, Japan

Background. Flow in individual vessels is passively determined when a single pump is used for selective cerebral perfusion during aortic arch surgery. We installed a Doppler flowmeter in the circuit and measured flow in the supraaortic vessels to determine flow distribution during selective cerebral perfusion.

Methods. We cannulated and perfused three supraaortic vessels using a single pump in 203 patients who underwent elective (n = 158) or emergency or urgent (n = 45) total arch replacement using a four-branched prosthetic graft. Flow rates in each branch were continuously monitored during selective cerebral perfusion.

Results. The respective mean flow rates in the brachiocephalic, left common carotid, and left subclavian arteries and total flow rates were 5.8, 3.3, 3.4, and 12.5 mL · kg^{-1} · min^{-1}. The ratios of flow in these vessels to total flow were 46.5%, 26.5%, and 27.0%, respectively, and

they were not affected by the total flow rate. In-hospital mortality rates among the patients who underwent elective and emergency or urgent surgery were 1.9% (n = 3) and 11.1% (n = 5), respectively, and the rates of postoperative stroke were 2.5% (n = 4) and 8.9% (n = 4), respectively. Total flow in the supraaortic vessels during selective cerebral perfusion was significantly lower in patients with neurologic complications than in those without (732 versus 806 mL/min; p = 0.034).

Conclusions. Flow monitoring showed that selective perfusion using a single pump adequately distributed flow among all supraaortic vessels. This monitoring system might help to improve brain protection and outcomes during total aortic arch replacement.

(Ann Thorac Surg 2013;95:29–35)
© 2013 by The Society of Thoracic Surgeons

A ortic arch surgery is challenging, and the key to success is protecting the brain. Selective antegrade cerebral perfusion (SCP) demands meticulous handling of the arch vessels compared with hypothermic circulatory arrest with or without retrograde cerebral perfusion. However, SCP confers the considerable advantage of not increasing the incidence of postoperative cerebral complications regardless of duration [1, 2], whereas brain protection by hypothermic circulatory arrest is seriously time-sensitive [3]. Most experimental and clinical studies have found that adding retrograde cerebral perfusion to hypothermic circulatory arrest does not confer any benefit [4–6].

We have perfused all three arch vessels with a single roller pump during aortic arch procedures since 1992. The flow in each branch is not individually controlled under these conditions. That is, only total flow can be controlled and flow distribution among the vessels is passively determined, which has led to concerns about whether the flow distribution is adequate. Our early experiences using this technique showed that monitoring

the perfusion flow rate through each arch vessel is necessary to detect imbalances in cerebral blood distribution [1]. However, flow distribution among the supraaortic vessels during SCP has not yet been described. We therefore installed a Doppler flowmeter in the SCP circuit and measured the blood flow in each supraaortic vessel during SCP. A constant perfusion temperature was maintained throughout SCP to minimize changes in cerebral metabolic demand. The present study aims to improve brain protection based on assessments of flow distribution during SCP using a single pump.

Patients and Methods

Our institutional review board approved this retrospective study, and individual consent was waived. Between January 2001 and November 2011, 347 patients underwent aortic arch surgery using SCP. Among them, 203 (159 men, 44 women; age, 27 to 84 years; elective, n = 158; urgent, n = 11; emergency, n = 34) underwent total arch replacement using a four-branched prosthetic graft while the flow of each supraaortic branch was measured during SCP. Thus, patients who underwent hemiarch or partial arch replacement with reconstruction of only one or two branches were not included in this series (Table 1).

Table 1. Patient Characteristics

Variable	Number	Ratio (%)
Number of patients (n)	203	
Age (y)		
Mean ± SD	67.9 ± 10.0	
Range	27–84	
Sex		
Male	159	78.3
Female	44	21.7
Marfan syndrome	3	
Etiology		
Aortic dissection	69	34.0
Nondissection	134	66.0
Elective[a]	158	77.8
Urgent[a]	11	5.4
Emergency[a]	34	16.7
Cardiac tamponade or shock	13	6.4
Coma	1	0.5
Preoperative morbidity		
Cerebrovascular disease[b]	46	22.7
Coronary artery disease[c]	61	30.0
Chronic obstructive pulmonary disease[d]	25	12.3
Diabetes mellitus	12	5.9
History of heart surgery	15	7.4
History of aortic surgery	43	21.2

[a] Elective is defined as routine admission for surgery; urgent is defined as patients requiring intervention or surgery on admission for medical reasons (these patients could not be discharged without a definitive procedure); emergency is defined as operation needed before the start of the working day after a decision to operate had been reached.   [b] History of cerebral infarction, transient ischemic attack, subarachnoid hemorrhage, stenosis of carotid artery (noninvasive ≥50%), or prior carotid surgery.   [c] History of myocardial infarction, coronary artery bypass, percutaneous coronary intervention, or significant coronary artery stenosis by preoperative coronary angiography.   [d] Forced expiratory volume in 1 second to forced vital capacity ratio less than 70%, or on chronic inhaled or oral bronchodilator therapy.

SD = standard deviation.

Operative Procedures

Patients were placed in the supine position for median sternotomy. The ascending aorta usually served as a cannulation site for arterial return, and the right axillary artery served as the site if atherosclerotic changes in the ascending aorta were severe or too large for safe cannulation or if aortic dissection was the presenting pathologic disease. The right auricular appendage was usually cannulated for venous drainage. Cardiopulmonary bypass was started, and the left ventricle was vented from the cannula through the right upper pulmonary vein. The patients were cooled using the alpha-stat method of pH control until the rectal or bladder temperature reached between 25° and 28°C. Hypothermic circulatory arrest was established, and the aorta was incised. Three supraaortic vessels were cannulated from their openings inside the incised aortic arch with balloon-tipped cannulas for SCP. The supraaortic vessels were reconstructed using only a polyethylene terephthalate fiber (Dacron)

graft with three branches for reconstruction and one for arterial return. All patients underwent open distal anastomosis, and the stepwise technique was applied for deep anastomoses [10]. This technique included the insertion of a short tube graft into the descending aorta, anastomosing it at the distal stump, extracting the distal end of the inserted graft, and proximally anastomosing a four-branched arch graft. Although this technique requires the additional step of anastomosing an interposed short prosthetic graft, it guarantees secure hemostasis and thus we prefer to use this technique. A left thoracotomy was added for 16 patients in whom aneurysms extended further distally and could not be approached from the median sternotomy. After completing distal anastomosis, air was removed from the abdominal and the descending aorta using the additional cannula in the femoral artery, and then systemic perfusion was resumed through the branch of the arch graft designed for arterial return. The supraaortic left subclavian, left common carotid, and brachiocephalic arteries were then reconstructed individually in this order. We have never applied en-bloc repair. Selective perfusion to each supraaortic vessel was continued during anastomosis until immediately before the corresponding vessel was reconstructed to minimize perfusion interruption. Selective cerebral perfusion was finally terminated just before reconstruction of the third branch, or the brachiocephalic artery, was completed, and then systemic physiologic warming was started, followed by anastomosis of the ascending aorta.

Concomitant procedures included coronary artery grafting (n = 41), aortic root replacement (n = 3), aortic valve replacement (n = 5), aortic valve resuspension (n = 19), mitral valve replacement (n = 1), tricuspid annuloplasty (n = 1), and aortic stent-graft (n = 5).

The durations of cardiopulmonary bypass, cardiac arrest, and SCP were 230 ± 62 (mean ± standard deviation), 151 ± 42, and 106 ± 26 minutes, respectively (Table 2).

Cerebral Perfusion Technique

The brains of all patients were protected by SCP during distal anastomosis and arch reconstruction. Circulatory

Table 2. Intraoperative Findings

Variable	Result
Pump run time (min; mean ± SD)	
Cardiopulmonary bypass	230 ± 62
Cardiac arrest	151 ± 42
Selective cerebral perfusion	106 ± 26
Concomitant procedures	
Coronary artery bypass grafting	41 (20.2%)
Aortic root replacement	3 (1.5%)
Aortic valve resuspension	19 (9.4%)
Aortic valve replacement	5 (2.5%)
Mitral valve replacement	1 (0.5%)
Stent-graft implantation	5 (2.5%)

SD = standard deviation.

arrest was established after the rectal or bladder temperature fell to between 25° and 28°C. All three supraaortic branches were cannulated and perfused through individual balloon-tipped cannulas (brachiocephalic, left carotid, and left subclavian arteries: 15F, 12F, and 12F, respectively) that diverged from the single side branch of the arterial return of the main circuit. All three branches were perfused using a single roller pump, and flow distribution was passively determined depending on the vascular resistance of each vessel. The initial total perfusion rate in supraaortic vessels was regulated to maintain at least at 10 mL $\cdot$ kg^{-1} $\cdot$ min^{-1}. The target pressure measured at the tip of the left carotid cannula was 30 to 50 mm Hg. When perfusion pressure fell to less than 30 mm Hg or increased to greater than 50 mm Hg, the flow rate was respectively increased to 18 mL $\cdot$ kg^{-1} $\cdot$ min^{-1} or initially decreased and followed with vasodilators if necessary. The target hematocrit value was between 20% and 25%. The patients were not warmed, and the perfusate temperature was maintained at a temperature lower than that of the rectum until supraaortic reconstruction with SCP was completed.

The perfusion rate of each supraaortic vessel during SCP was continuously monitored in real time using an ultrasound Doppler flowmeter (MedStim, Cleveland, OH) that was installed in the circuit next to a balloon-tipped perfusion cannula beforehand (Fig 1). The cephalad positioning of the flowmeters relative to the operative field ensured that surgical maneuverability was not compromised.

When the information changed significantly, for example, if the flow rate of one vessel fell abruptly while the other two increased, we considered the possibility of tube issues, such as kinking or malpositioning, and immediately examined the cannulas and resolved the matter if necessary.

Diagnosis and Classification of Neurologic Disturbances

All patients with postoperative neurologic disturbances were referred to a neurologist for examination by computed tomography or magnetic resonance imaging, or both. Postoperative cerebral complications were classified either as a temporary neurologic disturbance defined as a delay in awakening of greater than 24 hours or delirium with negative related focus in the brain and complete resolution before discharge, or as stroke defined as neurologic disturbances accompanied by new, documented focal brain lesions regardless of severity.

Statistical Methods

Predictive relationships among variables were determined using a simple linear regression analysis. Parametric variables were compared using Student's t test. Results are presented as mean $\pm$ standard deviation. Data were statistically analyzed using SPSS version 20.0 (SPSS, Chicago, IL). The significance level was set at a probability value of less than 0.05.
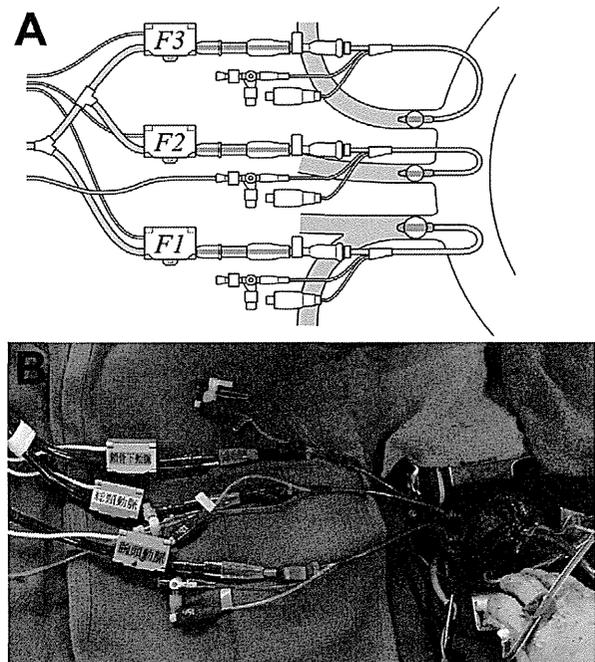

Fig 1. Selective antegrade cerebral perfusion. (A) Schema. (B) Photographed image. All three supraaortic vessels were cannulated by means of balloon-tipped cannulas positioned from their openings through the incised aorta and perfused using a single pump. Flow distribution was passively determined depending on the vascular resistance of each vessel. Ultrasound Doppler flowmeters (F1, F2, F3) were installed in the circuit next to balloon-tipped perfusion cannulas, and flow rates of supraaortic vessels were continuously measured in real time. Flowmeters were positioned cephalad to the operative field and did not affect maneuverability.

Results

Temperature, Pressure, and Flow During Selective Cerebral Perfusion

Rectal temperatures at the start of hypothermic circulatory arrest, 30 minutes thereafter, at the resumption of systemic perfusion and at the termination of SCP were 25.8° $\pm$ 2.7°C, 25.4° $\pm$ 2.4°C, 25.3° $\pm$ 2.0°C, and 26.1° $\pm$ 1.9°C, respectively (Fig 2). The perfusate was maintained at a lower temperature than the rectal temperature until SCP was complete. At 30 minutes after starting SCP, the perfusate temperature was 23.0° $\pm$ 2.2°C, the pressure of the top of the balloon cannula into the left carotid artery was 39.2 $\pm$ 10.3 mm Hg, the total flow of the three supraaortic branches measured using the flowmeter at the roller pump was 11.4 mL $\cdot$ kg^{-1} $\cdot$ min^{-1}, and flow rates in the brachiocephalic, left common carotid and left subclavian arteries and the total of these three vessels measured by Doppler flowmeter at the corresponding tube were 5.84 $\pm$ 1.31, 3.31 $\pm$ 0.74, 3.38 $\pm$ 0.86, and 12.5 $\pm$ 2.2 mL $\cdot$ kg^{-1} $\cdot$ min^{-1}, respectively. The flow in each supraaortic vessel was parallel to the total flow of the three vessels (Fig 3). The relationships between flow in the brachiocephalic, left carotid, and left subclavian arteries and total flow of the supraaortic vessels is described by the following
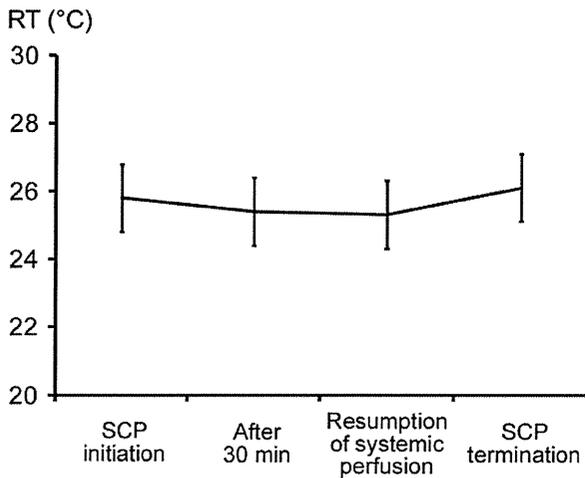
Fig 2. Rectal temperature during selective cerebral perfusion (SCP). Rectal temperatures (RT) at the start of hypothermic circulatory arrest, 30 minutes later, at resumption of systemic perfusion, and termination of selective cerebral perfusion were 25.8° ± 2.7°C, 25.4° ± 2.4°C, 25.3° ± 2.0°C, and 26.1° ± 1.9°C, respectively. Body temperature was maintained at a low level until selective cerebral perfusion was terminated.

regression equations: $y = 0.50x - 0.48$, $y = 0.25x + 0.22$, and $y = 0.25x + 0.26$, where y is the flow of the brachiocephalic ($R^2 = 0.68$; $p < 0.001$), left common carotid ($R^2 = 0.51$; $p < 0.001$), and left subclavian ($R^2 = 0.39$; $p < 0.001$) arteries, respectively, and x is the total flow of the supraaortic vessels. The proportion of flow among the three vessels was not affected by the total flow rate (Fig 4). The mean ratio of the flow of each vessel was 46.5% ± 6.1%, 26.5% ± 4.1%, and 27.0% ± 5.6% of the total supraaortic flow, respectively.

Clinical Outcomes

Three (1.9%) of 158 and 5 (11.1%) of 45 patients who underwent elective and emergency or urgent surgery died in hospital of pneumonia (n = 2), respiratory failure (n = 2), cerebral infarction (n = 1), arrhythmia (n = 1), sepsis (n = 1), and multiple organ failure as a result of acute aortic dissection (n = 1).

Tracheal tubes were removed within 24 hours from 120 patients, between 24 hours and 7 days from 71 patients, and after 7 days from 12 patients. Among 7 patients who required postoperative hemodialysis, 3 died before discharge and the remaining 4 were finally weaned from hemodialysis.

Postoperative stroke occurred in 8 (3.9%) patients; 4 each were scheduled for surgery (2.5%) and emergency or urgent surgery (8.9%) (Table 3). Temporary cerebral disturbances developed in 20 (9.9%) patients, 13 (8.2%) were scheduled for surgery, and 7 (15.6%) underwent emergency or urgent surgery. One patient experienced paraplegia after extensive repair through a median sternotomy and an additional left thoracotomy.

The total flow rate in the supraaortic vessels was significantly lower in 27 patients who experienced neurologic complications (1 patient was excluded because of severe preoperative brain damage) than in 175 who did not (732 ±

146 versus 806 ± 170 mL/min; $p = 0.034$). The total flow rate per body weight tended to be lower in patients with neurologic complications than in those without (11.8 ± 1.4 versus 12.6 ± 2.2 mL · kg^{-1} · min^{-1}), although the difference did not reach statistical significance ($p = 0.073$).
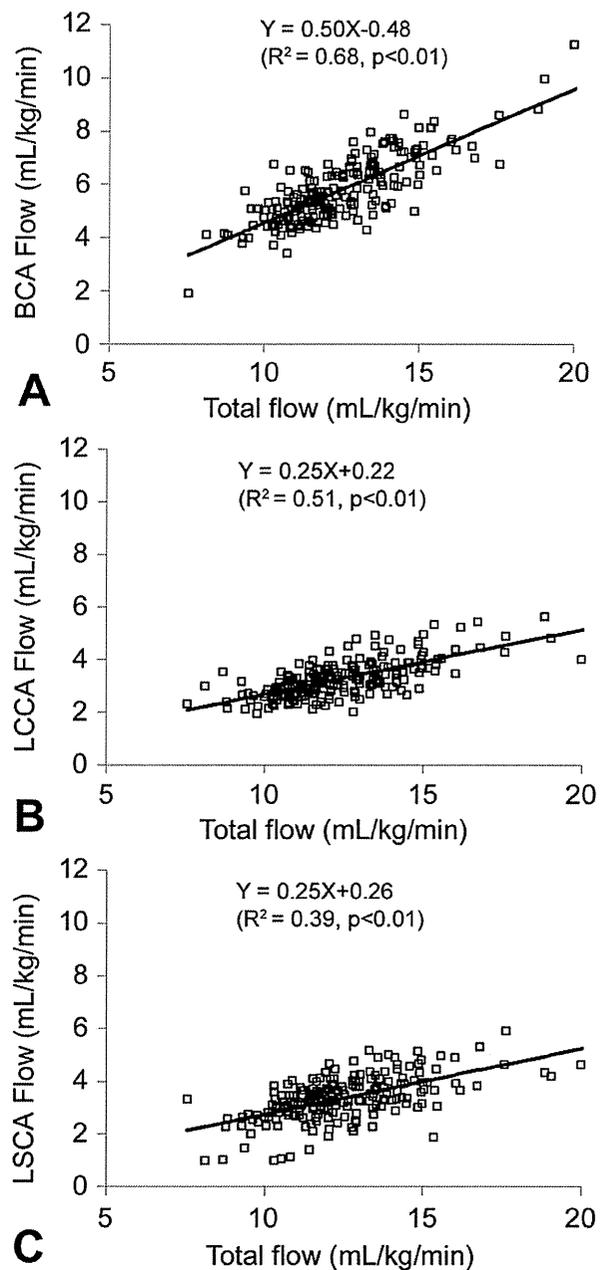

Fig 3. Flow rate of supraaortic vessels during selective cerebral perfusion. (A) Brachiocephalic artery (BCA). (B) Left common carotid artery (LCCA). (C) Left subclavian artery (LSCA). Flow in each supraaortic vessel was parallel to total flow of all three vessels. Relationships between flow in BCA, LCCA, and LSCA and total flow in supraaortic vessels are described by regression equations as given in the text.
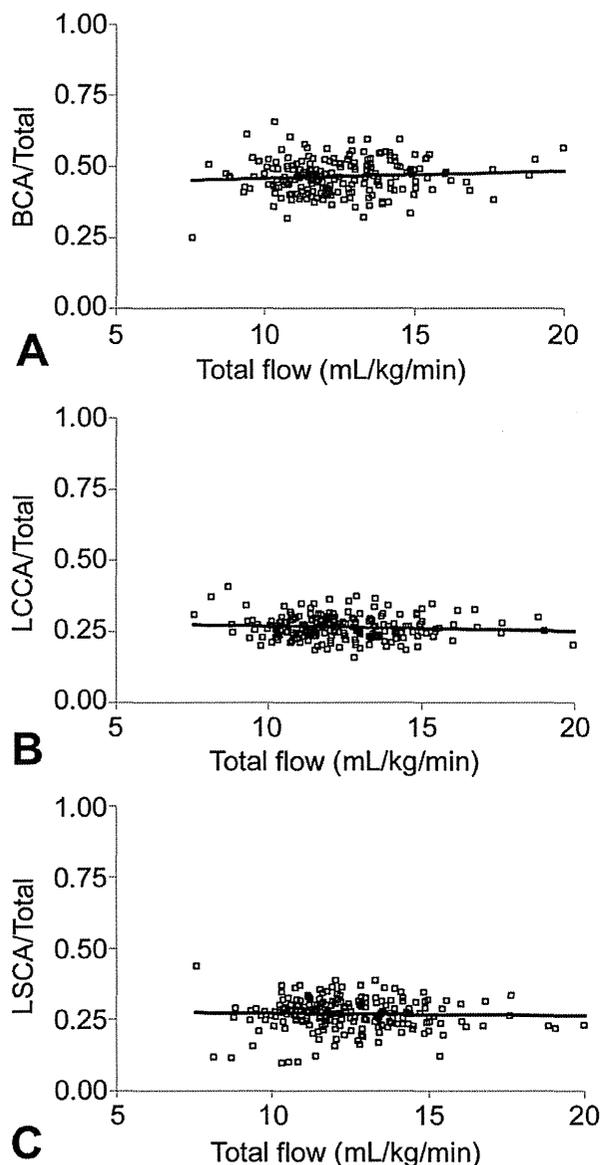
Fig 4. Proportion of flow in supraaortic vessels versus total flow. (A) Brachiocephalic artery (BCA). (B) Left common carotid artery (LCCA). (C) Left subclavian artery (LSCA). Total flow rate did not affect the proportion of flow in each supraaortic vessel.

Comment

Brain protection is one of the most important issues involved in achieving successful outcomes of aortic arch surgery. Antegrade cerebral perfusion is reportedly the most reliable measure that can be taken to protect the brain during aortic arch manipulation. Since 1992 we have perfused all three arch vessels with a single roller pump during aortic arch replacement. This system is simple and involves less priming volume than multiple-pump systems, although some surgeons recommend using two pumps to perfuse each brain hemisphere and

prevent maldistribution [7]. The single-pump system allows measurement of the total flow rate of supraaortic vessels and not that of each individual vessel. Our early experiences using this technique showed that the perfusion flow rate through each arch vessel required monitoring to detect imbalances in cerebral blood distribution [1]. We thus installed Doppler flowmeters in the circuit entering each of the three supraaortic vessels. The real-time flow rate of each vessel is displayed digitally, and it is easily visualized, although the flow rate of each vessel could not be individually regulated.

Our results showed that blood flow in the brachiocephalic artery that supplies the right hemisphere constituted an average of about half of the total flow of supraaortic vessels regardless of considerable individual variability. The supraaortic vessels were perfused by a single roller pump, and flow distribution in each was passively determined without artificial control. Although to our knowledge the normal range of supraaortic vessels has not been determined, Schoning and associates [8] reported that side-to-side differences in flow volumes of the common, external, and internal carotid arteries are not significant. Flow to the left carotid and left subclavian arteries averaged about 25% of the total supraaortic flow in each. The ratio of flow distribution in our series seemed reasonable and might be similar to the physiologic distribution.

Although the pressure at the tip of the cannula into the left carotid artery was relatively low (mean, 39.2 mm Hg), postoperative brain complications rarely occurred in our series. These findings were similar to a report indicating that brain perfusion is dependent on flow and scattered almost transversely to mean arterial pressure [9].

Total flow in the supraaortic vessels was significantly lower in patients with, than without postoperative neurologic complications. These results suggested that the total flow rate of supraaortic vessels during SCP is closely related to the incidence of postoperative cerebral complications. Tanaka and colleagues [10] suggested that the safe range of cerebral perfusion flow during moderate hypothermia at 25°C is about 10 mL $\cdot$ kg^{-1} $\cdot$ min^{-1} with a perfusion pressure (carotid arterial pressure) of about 30 mm Hg or greater, and this was extrapolated in an animal model. We found that a cerebral flow rate of 10 mL $\cdot$ kg^{-1} $\cdot$ min^{-1} is insufficient during SCP in humans when the body temperature during circulatory arrest reaches 25° to 28°C. A higher flow rate is recommended, although we could not define the optimal cerebral flow rate from the present data.

Measuring the flow of each vessel also conferred another advantage as an indication of trouble within the circuit. Flow sensors in arch vessels have often revealed either kinking or malpositioning of the perfusion catheter by indicating an abrupt reduction in the flow rate of one cannula with a simultaneous increase in the flow rate of the other two. During accidental cannula removal, flow in the corresponding branch abruptly increased and that in the other two branches decreased. We believe that such circuit trouble is a key factor involved in maldistribution during SCP. This system can help to promptly avoid such issues and

Table 3. Postoperative Stroke

Patient No.	Age (y)/ Sex	Timing of Surgery	Operative Procedures	Preoperative Morbidity	Outcome
1	64 M	Emergency (acute dissection)	TAR	Malperfusion, convulsion s/p AVR, s/p PMImp	IHD (Coma)
2	82 F	Emergency (acute dissection)	TAR	Cardiac tamponade, shock	Alive (full recovery)
3	60 M	Urgent (sealed rupture)	TAR + SG	Occlusion of VA/RtCCA, s/p CAB	IHD (craniotomy for decompression)
4	53 M	Urgent (subacute dissection)	TAR + AxA bypass		Alive (full recovery)
5	69 M	Scheduled	TAR + Bentall	CI	Alive (full recovery)
6	77 M	Scheduled	TAR	s/p OAAR, COPD	Alive (full recovery)
7	77 M	Scheduled	TAR	s/p CEA, CI, DM	Alive (hemiparesis)
8	73 M	Scheduled	TAR + CAB	CAD	Alive (monoplegia)

AVR = aortic valve replacement;   AxA = axillary artery;   CAB = coronary artery bypass grafting;   CAD = coronary artery disease;   CEA = carotid endarterectomy;   CI = cerebral infarction;   COPD = chronic obstructive pulmonary disease;   DM = diabetes mellitus;   IHD = in-hospital death;   OAAR = open abdominal aortic repair;   PMImp = pacemaker implantation;   RtCCA = right common carotid artery;   SG = stent-graft;   s/p = status post;   TAR = total arch replacement;   VA = vertebral artery.

might have contributed to the extremely low postoperative mortality and morbidity rates in this study.

Regional saturation of oxygen (INVOS; Somanetics, Troy, MI)) monitoring has become more frequent during arch surgery with antegrade brain perfusion. The present series of 80 (8 with and 72 without central nervous complications) patients underwent regional oxygen saturation monitoring. Regional oxygen saturation in the head did not significantly differ between the two groups (66.7% ± 12.4% versus 70.2% ± 10.7%; $p = 0.385$). A larger scale study is needed to explore this issue and to understand potential correlations among the three systems (flowmeter, cerebral arterial pressure, and INVOS).

Total arch replacement under selective perfusion of three supraaortic vessels using a single roller pump and monitoring the flow of each supraaortic vessel provided clinically acceptable brain protection and achieved low mortality and morbidity rates. Blood flow appears to be distributed adequately when all supraaortic vessels are perfused using a single pump during SCP. However, monitoring flow rates in each supraaortic vessel is recommended to detect kinking or malpositioning of the perfusion catheter. Flow rate during SCP is related to the incidence of postoperative cerebral complications.

References

1. Ueda T, Shimizu H, Ito T, et al. Cerebral complications associated with selective perfusion of the arch vessels. Ann Thorac Surg 2000;70:1472-7.

2. Kazui T, Washiyama N, Muhammad BA, Terada H, Yamashita K, Takinami M. Improved results of atherosclerotic arch aneurysm operations with a refined technique. J Thorac Cardiovasc Surg 2001;121:491-9.

3. Ergin MA, Galla JD, Lansman L, Quintana C, Bodian C, Griepp RB. Hypothermic circulatory arrest in operations on the thoracic aorta. Determinants of operative mortality and neurologic outcome. J Thorac Cardiovasc Surg 1994; 107:788-99.

4. Boeckxstaens CJ, Flameng WJ. Retrograde cerebral perfusion does not perfuse the brain in nonhuman primates. Ann Thorac Surg 1995;60:319-28.

5. Ye J, Yang L, Del Bigio MR, et al. Retrograde cerebral perfusion provides limited distribution of blood to the brain: a study in pigs. J Thorac Cardiovasc Surg 1997;114: 660-5.

6. Harrington DK, Bonser M, Moss A, Heafield MT, Riddoch MJ, Bonser RS. Neuropsychometric outcome following aortic arch surgery: a prospective randomized trial of retrograde cerebral perfusion. J Thorac Cardiovasc Surg 2003;126:638-44.

7. Ohmi M, Tabayashi K, Hata M, Yokoyama H, Sadahiro M, Saito H. Brain damage after aortic arch repair using selective cerebral perfusion. Ann Thorac Surg 1998;66:1250-3.

8. Schöning M, Walter J, Scheel P. Estimation of cerebral blood flow through color duplex sonography of the carotid and vertebral arteries in healthy adults. Stroke 1994;25: 17-22.

9. Soma Y, Hirotani T, Yozu R, et al. A clinical study of cerebral circulation during extracorporeal circulation. J Thorac Cardiovasc Surg 1989;97:187-93.

10. Tanaka H, Kazui T, Sato H, Inoue N, Yamada O, Komatsu S. Experimental study on the optimum flow rate and pressure for selective cerebral perfusion. Ann Thorac Surg 1995;59:651-7.

INVITED COMMENTARY

This study by Shimizu and colleagues [1] presents a large series of 203 patients undergoing total arch replacement by the use of antegrade selective cerebral perfusion (ASCP) and moderate hypothermia (25° to 28°C). The postoperative outcomes were remarkably good, as demonstrated by an elective hospital mortality of 1.9%, an elective stroke rate of 2.5%, and a severe renal failure rate

(hemodialysis) of 3.4%. Such results, for which the authors are to be commended, confirm once more that ASCP and moderate hypothermia represent the best method to protect the brain and other organs during total arch replacement operations.

In addition, the authors describe in detail their method and circuit for ASCP, which involves a dedicated single

大動脈疾患症例の実態解明・効果的な進行予防・治療を目的とした全国的統一基盤システムの構築と研究 研究班

区　　　　分	氏　　名	所　　属　　等	職　　名
研 究 代 表 者	鈴木亨	東京大学大学院医学系研究科ユビキタス予防医学講座	特任准教授
研 究 分 担 者	高本眞一	三井記念病院	病院長
	平田恭信	東京逓信病院	病院長
	本村昇	東京大学医学部附属病院心臓血管外科	准教授
	志水秀行	慶應義塾大学医学部心臓血管外科	講師
	古庄知己	信州大学医学部附属病院遺伝子診療部	准教授
	澤城大悟	東京大学医学部附属病院循環器内科	特任助教
研 究 協 力 者	宮田裕章	東京大学大学院医学系研究科医療品質評価学講座	教授
	宮入剛	三井記念病院心臓血管外科	教授
	竹谷剛	三井記念病院心臓血管外科	科長
	渡邉淳	日本医科大学附属病院遺伝診療科/生化学/分子生物学	准教授
	簑持淳	獨協医科大学皮膚科	教授
	森崎裕子	国立循環器病研究センター研究所分子生物学部	室長
事　　務　　局	木村亜紀子	〒113-8655 TEL　03-5800-9846 FAX　03-5800-9847 e-mail　ubiquitous-office@umin.net	
経理事務担当者	朝倉良夫 大溝真由美	〒113-8655 TEL　03-5800-9753 FAX　03-5800-9145 e-mail　Kenkyukyoryokuall@adm.h.u-tokyo.ac.jp	